


Article

The Predictive Model of Surface Texture Generated by Abrasive Water Jet for Austenitic Steels

Ján Kmec ¹, Miroslav Gombár ², Marta Harničárová ^{1,3,*}, Jan Valíček ^{1,3}, Milena Kušnerová ¹, Jiří Kríž ⁴, Milan Kadnár ⁵, Monika Karková ¹ and Alena Vagaská ⁶

¹ Institute of Technology and Businesses in České Budějovice/Department of Mechanical Engineering, Okružní 517/10, 370 01 České Budějovice, Czech Republic; kmec@mail.vstecb.cz (J.K.); jan.valicek@uniag.sk or valicek.jan@mail.vstecb.cz (J.V.); kusnerova.milena@mail.vstecb.cz (M.K.); karkova@mail.vstecb.cz (M.K.)

² Faculty of Management, University of Prešov in Prešov, Konštantínova 16, 080 01 Prešov, Slovak Republic; miroslav.gombar@unipo.sk

³ Department of Electrical Engineering, Automation and Informatics, Faculty of Engineering, Slovak University of Agriculture in Nitra, Tr. A. Hlinku 2, 949 01 Nitra, Slovak Republic

⁴ Institute of Informatics, Faculty of Business and Management, University of Technology, Kolejní 2906/4, 612 00 Brno, Czech Republic; kriz@fbm.vutbr.cz

⁵ Department of Machine Design, Faculty of Engineering, Slovak University of Agriculture in Nitra, Tr. A. Hlinku 2, 949 01 Nitra, Slovak Republic; milan.kadnar@uniag.sk

⁶ Department of Natural Sciences and Humanities, Faculty of Manufacturing Technologies with a Seat in Prešov, Technical University of Kosice, Štúrova 31, 080 01 Prešov, Slovakia; alena.vagaska@tuke.sk

* Correspondence: harnicarova@mail.vstecb.cz or marta.harnicarova@uniag.sk; Tel.: +420-387-842-193

Received: 12 April 2020; Accepted: 29 April 2020; Published: 1 May 2020



Abstract: Austenitic stainless steel belongs to the best oxidation-resistant alloys, which must function effectively and reliably when used in a corrosion environment. Their attractive combination of properties ensures their stable position in the steel industry. They belong to a group of difficult-to-cut materials, and the abrasive water jet cutting technology is often used for their processing. Samples made of stainless steel AISI 304 has been used as the experimental material. Data generated during experiments were used to study the effects of AWJ process parameters (high-pressure water volume flow rate, the diameter of the abrasive nozzle, the distance of the nozzle from the material surface, cutting head feed rate, abrasive mass flow, and material thickness) on surface roughness. Based on the analysis and interpretation of all data, a prediction model was created. The main goal of the long-term research was to create the simplest and most usable prediction model for the group of austenitic steels, based on the evaluation of the practical results obtained in the company Watting Ltd. (Budovateľská 3598/38, Prešov, Slovakia) during 20 years of operation and cooperation with customers from industrial practice. Based on specific customer requirements from practice, the publication also contains specific recommendations for practice and a proposal for the classification of the predicted cut quality.

Keywords: abrasive water jet; stainless steel; high-pressure water flow; abrasive mass flow; abrasive nozzle diameter; cutting head feed rate; material thickness; surface roughness

1. Introduction

As one of the rapidly developing unconventional machining methods, abrasive water jet technology (AWJ) has been steadily evolving since 1970 [1]. With its specific and unique advantages [2,3] such as good adaptability to different materials, no heat-affected zone, the low impact force on the workpiece, and favorable environmental impact, AWJ machining technology has become one of the advanced machining techniques. It has a good perspective application and improved competitiveness in modern

production [4]. A summary of applied research in recent years shows that AWJ is a versatile tool that is used in almost all manufacturing processes, such as cutting, milling, shaping, drilling, cleaning, and scaling [5].

In the AWJ machining process, ultra-high-pressure water is used to accelerate the abrasive particles sucked into the mixing chamber by the Ventury tube effect. Through the aperture and the focusing nozzle, the abrasive jet, in which the abrasive particles are carried is capable of cutting through, i.e., grind hard materials, results from high speed and energy. Because the combined action of erosion and impact wear of abrasive particles carried by the suspension through the focusing nozzle, the cut surface is formed in a unique shape that is different from other mechanical processing surfaces. It is well-known that the functionality of any product is influenced by surface topography. This method has a significant influence on surface texture. Monitoring of technological parameters of the cutting process is important in order to reach the required cutting depth, minimum roughness, and, last but not least, minimum economic cost.

The analysis of AWJ technology factors shows that the hydraulic factors (pressure, water orifice diameter) and the abrasive factors (kind of abrasive material, abrasive particle size, abrasive mass flow rate) have the greatest influence on the process of material cutting (its effectiveness and surface quality). Functional relations between these main surface structure parameters and regime parameters of AWJ technology were obtained and proved by many experimental results of numerous authors in both graphical and analytical form [6–16].

The research work of the authors [17–21] in the area of AWJ cutting is focused on three aspects: AWJ cutting tool geometry, mechanics of the cutting process, and material properties. The main result of their work was that they found a method for identification of a position of equilibrium/neutral plane in the cut produced by AWJ, and based on it, they determined the constant of material cuttability for abrasive water jet cutting technology [22,23].

In terms of a distinctive description in different areas, the cut surface has been divided into four zones designated as initiation zone, smooth zone, transition zone, and rough zone. In order to reveal details of the impact of the current on materials and the removal of workpiece materials, many experts have started to undertake further research on the friction and wear of abrasive particles on material surfaces. They have established some theoretical models [24] such as the “cutting-deformation”, “machining-deformation” model, elastic model, elastic-plastic model, etc.

The mechanism of formation of chips and the generation of traces after their removal are given by the trajectory of motion and the mechanism of the effect of particles. By sensing the motions by means of a high-velocity Charge-Coupled Device camera (CCD) camera on cuts in transparent materials, the mechanism of particle motion was studied by Hashish [25]. Hashish’s work is mostly associated with striation generation research. He developed a model to predict depths of cut that is based on a deep analysis of flow stress and a critical velocity [26]. A high-speed camera was also used by Orbanic and Junkar, who studied the macro mechanism of AWJ cutting and analyzed the formation of striations on the machined surface [27].

Machinability of nickel-based superalloy was studied by Uthayakuma et al. [28]. Experiments were conducted to analyze the influence of Abrasive Water Jet Machining parameters (AWJM) as follows (water jet pressure, feed rate of jet nozzle, and standoff distance) at three different levels on surface quality.

It was confirmed that the AWJ process is suitable for machining of difficult-to-cut materials. The work presented by Vasanth et al. provides detailed information on the choice of process parameters while machining titanium (Ti-6Al-4V) alloy [29]. The quality of the machined surface was significantly affected by the abrasive flow rate and standoff distance.

Another trend in research of AWJ cutting technology was to strengthen knowledge in the field of thermal energy distribution in the workpiece during cutting. For this purpose, the technique of infrared thermography was used [30]. Monitoring of thermal energy distribution in the cut when increasing the water pressure showed the effect of increasing the workpiece temperature and the heat

flux at the cut kerf. The peak temperature was reached near the cutting zone and was changing as the waterjet passed throughout the cut. Better understanding heat transfer and flow characteristics can be done by using models [31,32].

A comprehensive literature review has been recently done by [33]. It is a collection of knowledge in the field of AWJ from the period of 1960–2019. This review summarizes the references to the research providing the reader with sufficient insight and understanding to operate and improve high-quality and cost-effective AWJ machining operations.

The concerned searches also list the applications of AWJ technology for austenitic steel as the most widely used and applied material in the current market as high-quality stainless steel. The basic type of austenitic steels is AISI 304 steel, steel that has a low carbon content, so it is well weldable. When machining the surface with an AWJ beam, it is a cold cut, i.e., the material properties of the surface layer of the cut virtually do not change. Therefore, it can be stated that the presented measurements of steel type AISI 304 correspond to other types of austenitic steel. This material is characterized by excellent properties, has very good cold ductility, can be strengthened during forming, bends well, is well polishable, and can withstand temperatures up to 300–350 °C. Machinability is not good, but it is possible to machine with very sharp tools. This steel is especially resistant to water, water vapor, air humidity, edible acids, and weak organic and inorganic acids. For these reasons, it currently has a very wide range of applications. It is mainly used in the food and chemical industries, as well as in architecture and design [34].

The subject and main goal of this work are to create the simplest and most usable prediction model for a group of austenitic steels, based on the evaluation of practical results in the company Watting Prešov Ltd (Budovateľská 3598/38, Prešov, Slovakia) during 20 years of operation and cooperation with customers from industrial practice. Therefore, the publication focuses on the procedure of evaluating the *Ra* parameter as the mean arithmetic deviation of the profile.

Based on practical experience from experimental industrial applications for customers and knowledge of the prediction model, the classification of predicted quality represented by the *Ra* parameter of the surface at the given technological parameters of AWJ technology was also performed.

The publication also presents and recommends the experience gained from measuring, analyzing, and interpreting the results.

The next main aim of the article was to design and experimentally verify such technological parameters to maintain the quality of cutting of AISI 304 material, and to reduce the cost of the overall cutting process. The assumption was to increase production volume by 50%. Experimental research has been applied to the production of double-walled containers for liquid gases. In the presented paper, surface roughness is considered to be an important measure, since, in many industrial applications, it is a significant limitation of the applicability of the process. Further research work was needed to fully understand the impact of essential process parameters to achieve the desired steel surface roughness. Therefore, an experimental study was performed concerning the impact of the diameter of the abrasive nozzle (while maintaining a constant water jet diameter), water flow, abrasive mass flow, cutting head feed rate, and thickness of cut material for surface roughness of austenitic stainless steel AISI 304.

2. Materials and Methods

2.1. Material

The material of AISI 304 stainless steel was chosen because at the WATTING Prešov workplace, mostly the products of AISI 304 were cut in the volume of up to 70% of the monthly production. The processed material AISI 304 was used to verify the impact of the flow variation on the surface created by AWJ technology at a selected material thickness of 8 mm and a thickness of 30 mm. The material thickness of 8 mm and 30 mm was chosen deliberately for verification because of the practice requirements for cutting materials up to 30 mm thick, where this volume was almost 90% of the total cutting volume per year.

Characteristics of AISI 304 are given in Tables 1 and 2. An important property of the material is its toughness and good ductility.

Table 1. Chemical composition of AISI 304 [%].

C	Mn	Si	Cr	Ni	Mo	P	S
0.055	0.77	0.38	17.68	10.20	-	0.035	0.023

Table 2. Mechanical properties of AISI 304.

Mechanical properties	20 °C	50 °C	100 °C
Yield strength $R_{p0.2}$ [MPa]	≤ 186	≤ 177	≤ 157
Tensile strength R_m [MPa]		490–686	
Ductility A_5 [%]		≥ 50	
Notch strength $KCU 3$ [J·cm ⁻²]		≥ 196	
Hardness $HB 2.5/187.5$ [-]		220	

2.2. The Methodology of Experimental Tests

From the above-mentioned possibilities of combinations of high-pressure water flow and proportions of combinations of the abrasive focusing nozzle to the water nozzle, the shape of the test sample was cut, and the parameters important from the practical point of view were evaluated. The proposed test sample with the cutting direction is shown in Figure 1.

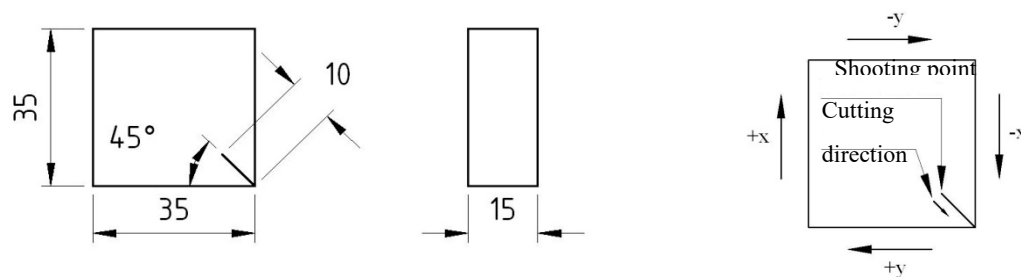


Figure 1. Test sample with the determination of the cutting direction.

Based on practical experience with water jet technology, the logistic sequence of cutting the test sample according to Table 3 was determined. The entire experimental study was then divided into four units. Table 4 presents data on the main cutting parameters, and Table 5 the secondary parameters for cutting the test samples.

Table 3. The logistic sequence of cutting the test sample.

Operation Order Number	Operation
1.	Make a shoot in the sample.
2.	In the sample, the cut length is 10 mm to measure the cutting gap so that it does not interfere with the cutting edge of the sample.
3.	Cut the sample in square shape.
4.	Cut each side of the square at a different speed, i.e., each sample contains four different cutting speeds.

Table 4. Data and main cutting parameters of the test sample.

Parameter Number	Parameter
1.	The distance of the nozzle from the material: 3; 5 mm.
2.	Abrasive nozzle diameter: 0.76; 1.02 mm.
3.	Volume flow rate: 1.05; 1.65; 2.37; 3.25 l·min ⁻¹ .
4.	Abrasive mass flow: 100; 150; 200; 250; (+300 and +330) g·min ⁻¹ .
5.	Cutting head feed rate: 50; 75; 100; 125 mm·min ⁻¹ .
6.	The thickness of the material being cut: 15 mm.

Table 5. Additional secondary cutting parameters of the test sample.

Parameter Number	Parameter
7.	High-pressure water pressure: 300 MPa.
8.	Water nozzle diameter: 0.20; 0.25; 0.30; 0.35 mm.
9.	Measured surface roughness <i>Ra</i> .

Figure 2 shows the sample cutting. The KMT Waterjet SL-VI 50 STD OA (KMT, Butzbach, Germany) high pressure pump was used for cutting (CNC X-Y table 3000 × 1500 mm; AUTOLINE I cutting head).

**Figure 2.** Cutting of test samples.

In order to define the cutting parameters of the test samples, constant and variable parameters were determined at their test cuts. Measured parameters were also defined on cut samples, which were comprehensively evaluated in a second separate experimental unit.

A total of 820 test cuts were performed on 77 test samples, including verification cuts. The total range of basic tests at a material thickness of 15 mm was 768 test cuts. These test cuts were performed on 64 samples, each sample being cut three times and at four cut sides.

The total range of the verification tests at a material thickness of 8 mm was 36 test cuts. These test cuts were made on identical square samples of the same material, namely for nine samples at four cut sides. The total range of verification tests at a material thickness of 30 mm was 16 test cuts. These test sections were made on identical square samples of the same material in terms of quality, namely for four samples, where four sides were cut.

For the presentation of experimental research, 16 samples were selected with the following numerical designations: 1-123-50; 5-123-50; 9-123-50; 13-123-50; 18-123-75; 22-123-75; 26-123-75; 30-123-75; 35-123-100; 39-123-100; 43-123-100; 47-123-100; 52-123-125; 56-123-125; 60-123-125; 64-123-125 (Table 6).

Table 6. The final collection of test sample cutting data [R/A/P—variables].

Sample Number	Distance of the Nozzle from the Material L	Water Nozzle Diameter d_o	Abrasive Nozzle Diameter d_a	Volume Flow Q_v	Abrasive Mass Flow m_a	Cutting Head Feed Rate v_p	Roughness R_a
	[mm]	[mm]	[mm]	[l·min ⁻¹]	[g·min ⁻¹]	[mm·min ⁻¹]	[μm]
1-123-50	3	0.20	1.02	1.05	100	50	9.34
18-123-75	3	0.25	1.02	1.65	150	75	12.65
35-123-100	3	0.30	1.02	2.37	200	100	13.05
52-123-125	3	0.35	1.02	3.25	250	125	16.96
5-123-50	5	0.20	1.02	1.05	100	50	9.94
22-123-75	5	0.25	1.02	1.65	150	75	13.85
39-123-100	5	0.30	1.02	2.37	200	100	17.05
56-123-125	5	0.35	1.02	3.25	250	125	19.86
9-123-50	3	0.20	0.76	1.05	100	50	9.34
26-123-75	3	0.25	0.76	1.65	150	75	12.65
43-123-100	3	0.30	0.76	2.37	200	100	14.73
60-123-125	3	0.35	0.76	3.25	250	125	18.74
13-123-50	5	0.20	0.76	1.05	100	50	7.37
30-123-75	5	0.25	0.76	1.65	150	75	8.71
47-123-100	5	0.30	0.76	2.37	200	100	15.15
64-123-125	5	0.35	0.76	3.25	250	125	16.98

2.3. Measurement of Surface Roughness of Dividing Surfaces Generated by AWJ

As a result of the AWJ process, the mean arithmetic deviation of the surface roughness profile R_a was chosen as the investigated quality parameter of the cut generated. The roughness along the central line is evaluated traditionally, as the average roughness at each level of the depth of cut. The roughness along the section of the nozzle inlet to the nozzle outlet is not monitored; it is theoretically assumed to be oscillating (reference). This parameter was measured by the Surftest SJ-301 tactile profilometer (Figure 3), which works on the principle of sensing the surface to be evaluated by a probe tipped with a diamond tip with a radius of curvature of 5 μm , located on the spring arm. Using the Surftest SJ-301, it is possible to evaluate the surface quality by various parameters according to different international standards, such as ISO 97, DIN 90, JIS 94, ANSI 95.

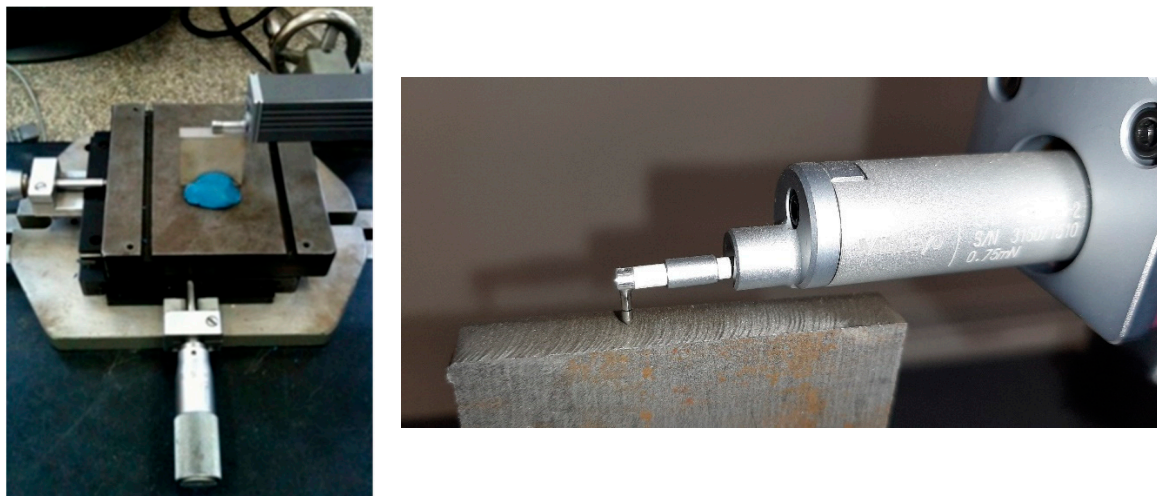


Figure 3. Measurement of the parameter of interest: (a) Position of the sample on a metal plate; (b) measuring the surface roughness at the center of the sample cut surface (detail).

The Surftest SJ-301 profilometer settings for sample measurements were:

- Evaluation standard: STN EN ISO 4287,
- Measured profile: R ,
- Parameter: R_a ,
- Filter: GAUSS,
- Boundary wavelength of the profile filter (cut-off): 2.5 mm,
- Number of sections measured: 5,
- Total measured length: 12.5 mm,
- Resolution: 0.01 μm (10 bites).

With regard to the fact that the monitored input quantities that affect the uncertainty associated specifically with 2D measurement of surface texture, it can be stated that the source of measurement errors is most often the measuring device itself and its software, as well as the measured surface properties and conditions under which the measurements are performed. In order to increase the accuracy of the measurement, visual inspection was performed during sample preparation, as well as cleaning of the sample from impurities with an alcohol-based liquid (cleaning from possible dust and grease). Fixation of the sample with plastic material and comparative fixation in a clamping device were also selected. The difference between the two variances of the measured values of roughness R_a did not exceed 3%. In order to increase the accuracy of the measurements, the identical orientation of the sample was also monitored in all repeated measurements. Only significant lines at a lateral distance of 0.1 mm were measured, and the influence of the positional effect was not demonstrated if the above measures were met.

2.4. Procedure for Researching and Retrieving Experimental Data

The first series of data collection was processed into protocols that were issued for each test sample being cut.

The second series of data collection was processed from the first series of data collection, with emphasis on concentrating data from three cases of sample cutting and concentrating sample data according to the state of the three main factors:

1. [flow, abrasive—variables; R speed—constant],
2. [flow rate, speed—variables; A abrasive—constant],
3. [abrasive, speed—variables; P flow—constant].

The third series of data collection was processed from the second series of data collection where the mean roughness values Ra were measured and recorded from three cases of cutting to determine the mean of the roughness value Ra from the three measured values. For each variant of the combination of variables, a new roughness measurement was always performed, resulting in negligible differences in measurements.

The fourth series of data collection is the final analysis for the final evaluation of the measured parameters of each sample in relation to the mean roughness value Ra , in relation to the stroke of the cutting head above the material and in relation to the inside diameter of the abrasive nozzle. The focus in the final evaluation was on processing according to the above-mentioned options, which is defined and reported by the second series of data collection. Examined parameters, their subsequent processing and preparation for their evaluation are shown in Table 6.

2.5. Statistical Modelling by Regression Analysis

In this subchapter, test and regression analysis are presented as methods to obtain a prediction model.

Kruskal–Wallis Test

This is a nonparametric alternative to Fisher's analysis of variance (ANOVA). The Kruskal–Wallis test is a generalization of the nonparametric Mann–Whitney test for more than two groups being compared. Like the Mann–Whitney test, it does not test the consensus of specific parameters, but the consensus of the selected distribution functions of the compared files, with the key assumption being the independence of the compared values. If k is the number of compared selections, the null and alternative hypotheses of the Kruskal–Wallis test are expressed as (1), (2):

$$H_0 : F_1(x) = F_2(x) = \dots = F_k(x) \quad (1)$$

$$H_1 : F_1(x) = F_2(x) = \dots \neq F_k(x) \quad (2)$$

The alternative hypothesis H_1 according to Equation (2) represents the fact that at least one F_i is different from the others. The main idea of the Kruskal–Wallis test is that under the validity of H_0 , the combined values from all samples are so well mixed that the average orders that correspond to the individual groups are similar [35,36]. When calculating the test, all observations are sorted by order (as if they came from one selection), and we assign an order to the individual values (R_{ij} will indicate the order of the j -th value in the i -th group). Let k be the total number of groups and n the total number of observations and n_1, n_2, \dots, n_k the number of observations in individual groups ($n = n_1 + n_2 + \dots + n_k$). Next, let us denote T_{ij} as the sum of the orders in the i -th group (3):

$$T_i = \sum_{j=1}^{n_i} R_{ij} \quad (3)$$

then the test statistic of the Kruskal–Wallis test will take the form (4):

$$Q = \frac{12}{n(n+1)} \sum_{i=1}^k \frac{T_i^2}{n_i} - 3(n+1) \quad (4)$$

It applies that the test statistic Q has a probability distribution with the parameter $k - 1$ under the validity of the null hypothesis (H_0) χ^2 (chi-square). We then reject the null hypothesis at the significance level α if the realization of the test statistic Q is higher than the critical value (quantile) corresponding to the significance level α , i.e., if (5):

$$Q \geq \chi_{k-1}^2(\alpha) \quad (5)$$

Statistical modelling by regression analysis was applied to create a complex dependence of the experimentally investigated factors of the AWJ process on the surface roughness value Ra . The basic results for the searched dependency in a general form can be expressed by Equation (6):

$$\hat{y} = b_0.x_0 + \sum_{j=1}^N b_j.x_j + \sum_{\substack{u,j=1 \\ u \neq j}}^N b_{uj}.x_u.x_j + \sum_{\substack{u,j=1 \\ u \neq j}}^N b_{uj}.x_u^2.x_j + \sum_{\substack{u,j=1 \\ u \neq j}}^N b_{uj}.x_u.x_j^2 + \sum_{j=1}^N b_{jj}.x_j^2 \quad (6)$$

where Ra , b_0 , b_j , b_{uj} , b_{jj} are the relevant regression coefficients, and x_j is the relevant independent variable; x_1 represents nozzle-to-material distance [mm], x_2 abrasive nozzle diameter [mm], x_3 volume flow rate [$\text{l} \cdot \text{min}^{-1}$], x_4 abrasive mass flow [$\text{g} \cdot \text{min}^{-1}$], x_5 cutting head feed rate [$\text{mm} \cdot \text{min}^{-1}$], and x_6 thickness of the material being cut [mm] (Table 7).

Table 7. Suitability of the model used.

Term	Value
RSquare	0.674
RSquare Adj	0.630
Root Mean Square Error	1.858
Mean of Response	8.217
Observations (or Sum Wgts)	68.000

In order to create a predictive model, only significant predictors and their interactions at the selected level of significance $\alpha = 0.05$ are considered, while the evaluation of their statistical significance was performed on the basis of the Student's t -test (7):

$$t(b_j) = \frac{b_j}{s(b_j)} \quad (7)$$

The standard deviation of the regression coefficient b_j is the square root of the variance (8):

$$s(b_j) = \sqrt{s^2(b_j)} \quad (8)$$

If inequality applies (9):

$$|t(b_j)| \geq t\left(1 - \frac{\alpha}{2}, n - p - 1\right) \quad (9)$$

where $t\left(1 - \frac{\alpha}{2}, n - p - 1\right)$ is the quantile of the Student's t -distribution, we reject the hypothesis of the statistical insignificance of the regression coefficient.

The results show that the predictive power of the model expressed by the adjusted index of determination is 62.96%. Thus, the model cannot explain 37.04% of the variability of the surface

roughness parameter Ra . The average surface roughness value Ra is 8.22 μm , with an average error of 1.36 μm .

From the variance analysis table (Table 8), it can be concluded that the variability due to random errors is significantly lower than the variability of the measured values explained by the model.

Table 8. ANOVA table of the model used.

Source	DF	Sum of Squares	Mean Square	F Ratio	Prob > F
Model	8	421.036	52.630	15.238	<0.0001
Error	59	20.778	3.454		
C. Total	67	624.814			

Testing the null (H_0) statistical hypothesis that results from the nature of the Fisher-Snedecor test criterion suggests that none of the effects used in the model has any effect on the significant change in the studied variable. It follows that the achieved significance level (Prob > F) is lower than the selected significance level ($\alpha = 0.05$). Therefore, it can be concluded that we do not have enough evidence to accept H_0 and claim that the model is adequate and significant. This means that adequate input variables have been chosen to describe the change in the roughness value Ra .

Further testing of the used model was carried out using the so-called Lack of Fit test for the model, i.e., the scattering of the residues and the scattering of the measured data within the groups were tested. This tests whether the regression model adequately reflects the observed dependence (Table 9).

Table 9. Lack of Fit test for the model.

Source	DF	Sum of Squares	Mean Square	F Ratio	Prob > F	Max RSq
Lack of Fit	35	118.874	3.396	0.960	0.552	0.864
Pure Error	24	84.904	3.538			
Total Error	59	203.778				

Given a significance level of 0.5522 by the Fisher test, the null statistical hypothesis that follows from the nature of the Lack of Fit test for the model can be accepted for the observed variable Ra , and it can be argued that the model sufficiently describes the variability of experimentally obtained data at a significance level of 5%.

Based on the above assumptions and their fulfilment (Tables 8 and 9), the following table (Table 10) represents an estimate of the parameters of the model with significance testing of individual effects and their combinations at the significance level $\alpha = 0.05$.

Table 10. Estimation of model parameters.

Term	Estimate	Std Error	t Ratio	Prob > t	Lower 95%	Upper 95%
Intercept	9.551	4.309	2.22	0.0305 *	0.929	18.174
x_1	−1.841	1.034	−2.08	0.0401 *	−3.910	0.228
x_5	0.052	0.008	6.43	<.0001 *	0.036	0.068
x_6	−0.074	0.029	−2.56	0.013 *	−0.133	−0.016
$x_1 * x_5$	−0.092	0.019	−4.83	<.0001 *	−0.130	−0.054
$x_1 * x_5 * x_5$	−0.002	0.001	−2.09	0.041 *	−0.003	−7.76·10 ^{−5}
x_3	0.703	0.697	2.01	0.047 *	−0.692	2.097
x_4	0.004	0.006	2.00	0.049 *	−0.007	0.016
$x_3 * x_4$	0.003	0.014	1.98	0.043 *	−0.024	0.030

* significant at a significance level of 5%.

3. Results and Discussion

3.1. Evaluation of Measurement Results from the Technological Point of View

Final evaluation of measured parameters on individual samples was realized on the basis of the analysis of the samples being cut and their subsequent processing. Such evaluation in relation to the mean roughness value Ra , in relation to the stroke of the cutting head above the material and in relation to the internal diameter of the abrasive nozzle was processed according to four categories (measured mean value Ra represents another variable, each roughness measurement always being a new measurement):

1. [flow, abrasive, roughness—variables; speed—constant],
2. [flow, velocity, roughness—variables; abrasive—constant],
3. [abrasive, speed, roughness—variables; flow—constant],
4. [flow, speed, abrasive, roughness—variables].

The subsequent evaluation of the samples is focused on the main cutting parameters, such as cutting speed, abrasive weight, and high-pressure water flow, in relation to the cut surface quality.

Conclusions of evaluated measurement results for the combination of variable flow rate, speed, abrasive, roughness are:

The following factors have a positive influence on the quality of the cut surface:

- Lower cutting speed 50 and 75 mm·min⁻¹,
- Lower cutting head lift above the material 3 mm,
- Abrasive nozzle, internal diameter 0.76 mm,
- Abrasive weight 150, 200 and 250 g·min⁻¹,
- The high-pressure water flow rate of 1.05 and 1.65 l·min⁻¹,
- The roughness of the cut surface can be achieved in the range of 6.2–15.8 µm,
- The overall roughness of the cut surface can be achieved in the range of 5–19 µm.

The quality of the cut surface is negatively influenced by:

- Higher cutting speed of 100 and 125 mm·min⁻¹,
- Higher cutting head lift over material 5 mm,
- Abrasive nozzle, internal diameter 1.02 mm,
- Weight of abrasive 200–250 g·min⁻¹,
- The high-pressure water flow rate of 2.37 and 3.25 l·min⁻¹,
- The roughness of the cut surface can be achieved in the range of 6.5–20 µm,
- The overall roughness of the cut surface can be achieved in the range of 6.5–27 µm.

The presented article is devoted to the analysis of the impact of basic factors as a separate effect; the next section addresses the impact of all input factors as a whole, in order to create a mathematical–statistical model. Experimental data related to the center of cut on the cut surface for each sample are used in the discussion, and the surface roughness is assessed based on the Ra parameter.

In AWJ cutting, increasing the speed of the cutting head reduces the number of abrasive particles that pass through the jet area unit. Accordingly, there are fewer impacts of cutting edges of abrasive particles per area unit, which ultimately leads to the formation of surfaces with a higher roughness value Ra (Figure 4).

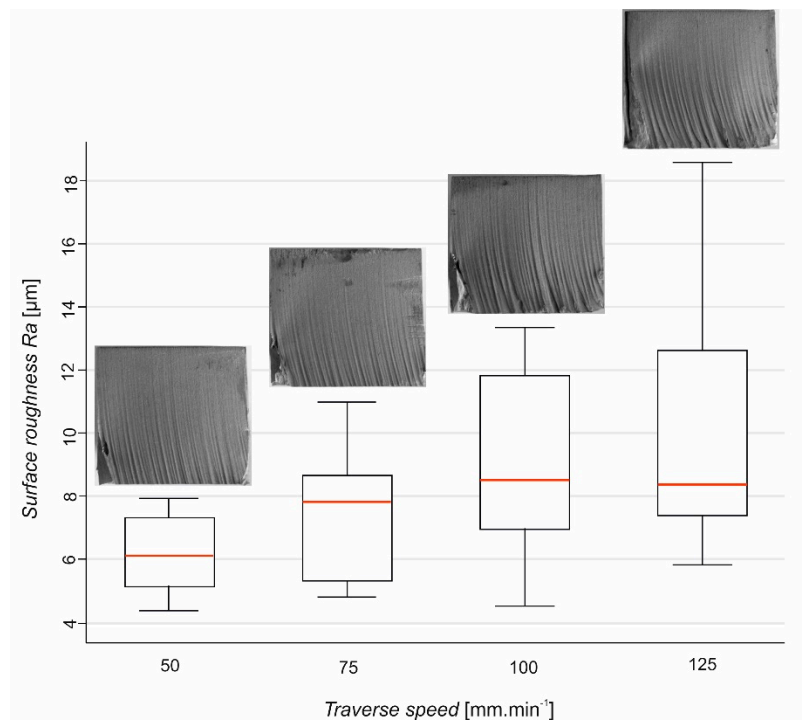


Figure 4. Effect of cutting head feed rate on the surface roughness value Ra .

The presented article is focused on high-pressure water flow, abrasive mass flow, and the internal diameter of the abrasive nozzle. Hydraulic parameters determine the hydraulic power of the abrasive water jet cutting and are based on the principle of fluid mechanics theory. The liquid pressure in the high-pressure water jet process is determined by the Bernoulli Equation (10) for the flow of incompressible liquid (10):

$$v^2 = \frac{2 \cdot p}{\rho} \quad (10)$$

where v [$\text{m}\cdot\text{s}^{-1}$] is the flow rate and ρ [$\text{kg}\cdot\text{m}^{-3}$] the density of the liquid medium. The pressure of the liquid is proportional to the square of the cutting speed, which is proportional to the kinetic energy of the particle of mass m . As a result, the water jet pressure determines the precise kinetic energy of the particle in the water jet. At higher pressures, the average kinetic energy of the water molecules is higher and more easily break the molecular bonds in the workpiece material. If the water pressure is adequate for cutting and for a given material while coherence is maintained, the material removal rate is determined by the flow coefficient.

3.2. Evaluation of Measurement Results from the Mathematical–Statistical Point of View

When analyzing the individual cutting speeds used and their effect on the change in the surface roughness value Ra using the non-parametric Kruskal–Wallis analysis of variance (Table 11), it can be said that $(H3, N = 68) = 15.05391$ the cutting head feed rate is a significant factor affecting the change in surface roughness ($p = 0.0018$). The value $p = 0.0018$ represents the result of the Kruskal–Wallis analysis of variance for the compared groups of feed rate: 50 [$\text{mm}\cdot\text{min}^{-1}$], 75 [$\text{mm}\cdot\text{min}^{-1}$], 100 [$\text{mm}\cdot\text{min}^{-1}$], 125 [$\text{mm}\cdot\text{min}^{-1}$] of the investigated parameter Ra in the probability scale. Given the chosen value of the significance level $\alpha = 0.05$, we reject the null statistical hypothesis, which follows from the nature of the Kruskal–Wallis test, and we can say that there is at least one sample (feed rate) that is statistically different from the others.

Table 11. Results of Kruskal–Wallis scattering analysis for cutting head feed rate.

Feed Rate [mm·min ^{−1}]	Valid [N]	Sum of Ranks	Mean Rank
50	17	350.500	20.618
75	17	535.500	31.500
100	17	713.000	41.941
125	17	747.000	43.941

Further analysis by multiple comparisons of p values shows that the statistically significant difference in surface roughness value Ra is 50 mm·min^{−1} and 100 mm·min^{−1}. Thus, an increase in the speed of 50 mm·min^{−1} causes an increase in the surface roughness value of Ra by 31.5%. The second statistically significant difference in surface roughness value Ra is 50 mm·min^{−1} and 125 mm·min^{−1}, respectively. Increasing the speed by 70 mm·min^{−1} will increase the surface roughness Ra by 37.1%. The difference between the surface roughness value Ra at the cutting head feed rate of 100 mm·min^{−1} and 125 mm·min^{−1} is 8.21%, but this difference is not significant at a significance level of 5%.

With AWJ cutting technology, increasing the flow rate increases the erosion efficiency, assuming a higher number of abrasive particles involved in the cutting process itself. Increasing abrasive mass flow means a relative increase in the depth of cut and on the other hand, a decrease in the surface roughness value (Figure 5b). Increasing the abrasive mass flow from 100 g·min^{−1} to 150 g·min^{−1} will result in a 14.6% reduction in surface roughness. A further increase in abrasive mass flow to 200 g·min^{−1} results in an 11.8% reduction in surface roughness. Within the range of experimentally used abrasive mass flow values, the surface roughness value decreased by almost 40.5% compared to the lower and upper limits. In the case of water flow and water pressure, increasing the pressure increases the kinetic energy of the individual particles within the stream, thereby improving the ability of the abrasive particles to remove the material. On the other hand, increasing water flow and pressure can lead to random collisions between particles inside the stream, to accelerating them and also to an increase in energy, which ultimately leads to surfaces with a higher roughness value (Figure 5a).

Increasing the current effective diameter in relation to the nozzle diameter can cause a loss of kinetic energy, resulting in surfaces with a higher roughness value (Figure 6).

The table of model parameters estimation (Table 11) shows that the change in the values of the investigated parameter in the range of experimentally used input variables has a significant effect on the significance level of 5% nozzle distance from the material, the effect of this input study variable on the overall variability of Ra being 8.67%. Furthermore, it can be concluded that increasing the distance of the nozzle from the material increases the conditional value of surface roughness Ra . Another significant input parameter that affects the surface roughness value is the cutting head feed rate with an overall effect on Ra variability of 26.81%. As the cutting head feed rate increases, the surface roughness value Ra also increases, which corresponds to the above results (Figure 4). The interaction of the distance between the nozzle and the material and the cutting head feed rate is also statistically relevant, with a 20.14% effect on the change in surface roughness value Ra . Equally significant is the effect of high-pressure water flow, with an 8.38% impact on the change in the roughness value Ra , abrasive mass flow with an 8.34% effect on the variability of Ra , and their interaction with 8.26% effect on the change in surface roughness value Ra . The thickness of the cut material, as the last statistically significant factor, affects the change in surface roughness value Ra by 10.68%. In this case, the influence of the diameter of the abrasive nozzle proved to be statistically insignificant, but this may be due to the interval of experimental input parameters used.

Based on the above, the regression dependence can be predicted (10):

$$Ra = 31.733 + 4.832 \cdot 10^{-2} \cdot x_3 - 7.428 \cdot x_1 - 1.173 \cdot 10^{-3} \cdot x_4 - 0.775 \cdot x_5 - 7.435 \cdot 10^{-2} \cdot x_6 + 0.219 \cdot x_1 \cdot x_5 + 3.224 \cdot 10^{-3} \cdot x_3 \cdot x_4 - 1.780 \cdot 10^{-3} \cdot x_1 \cdot x_5^2 + 6.701 \cdot 10^{-3} \cdot x_5^2 \quad (11)$$

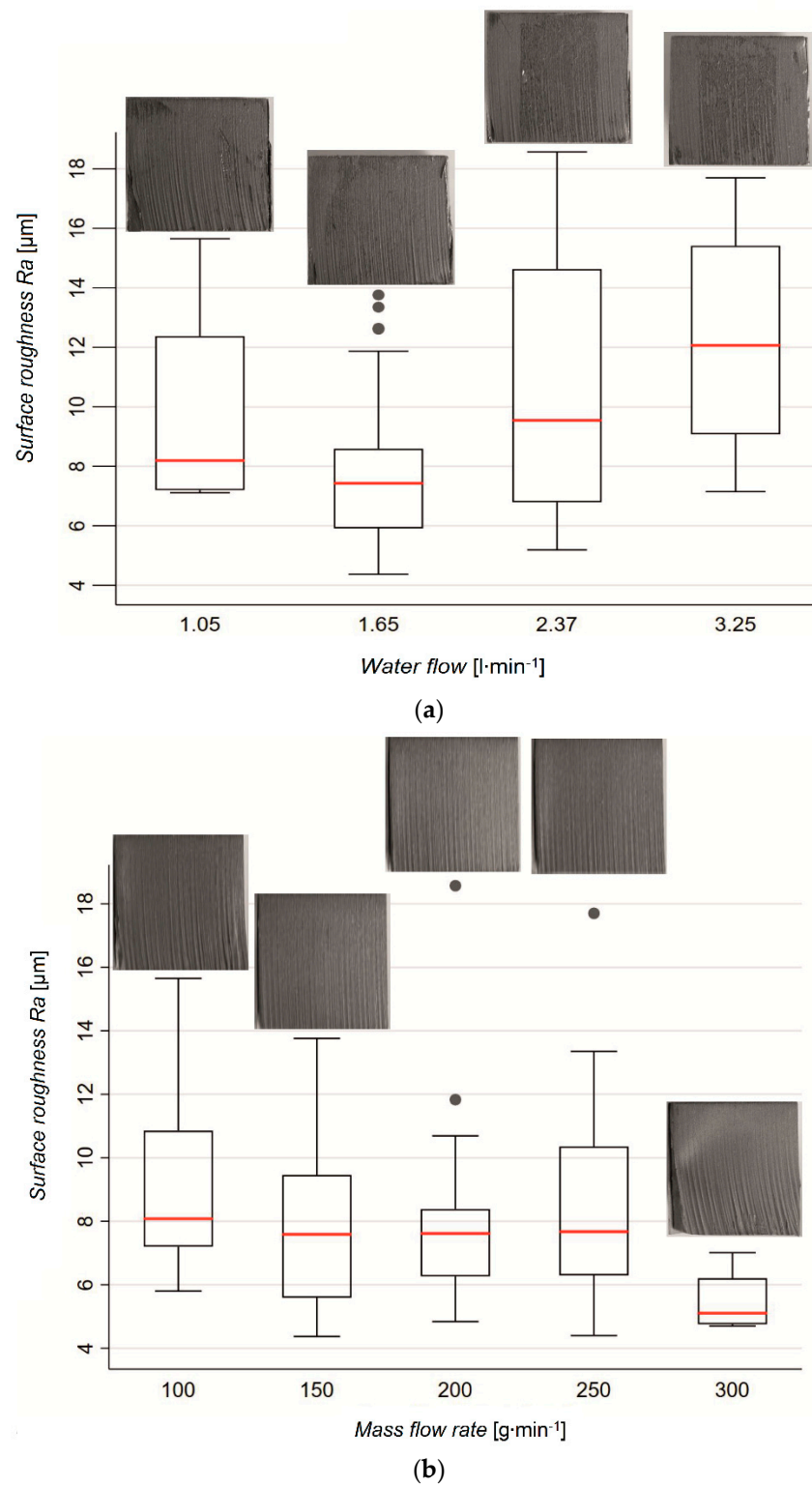


Figure 5. Effect of high-pressure water flow (a) and abrasive mass flow (b) on the change in surface roughness value R_a .

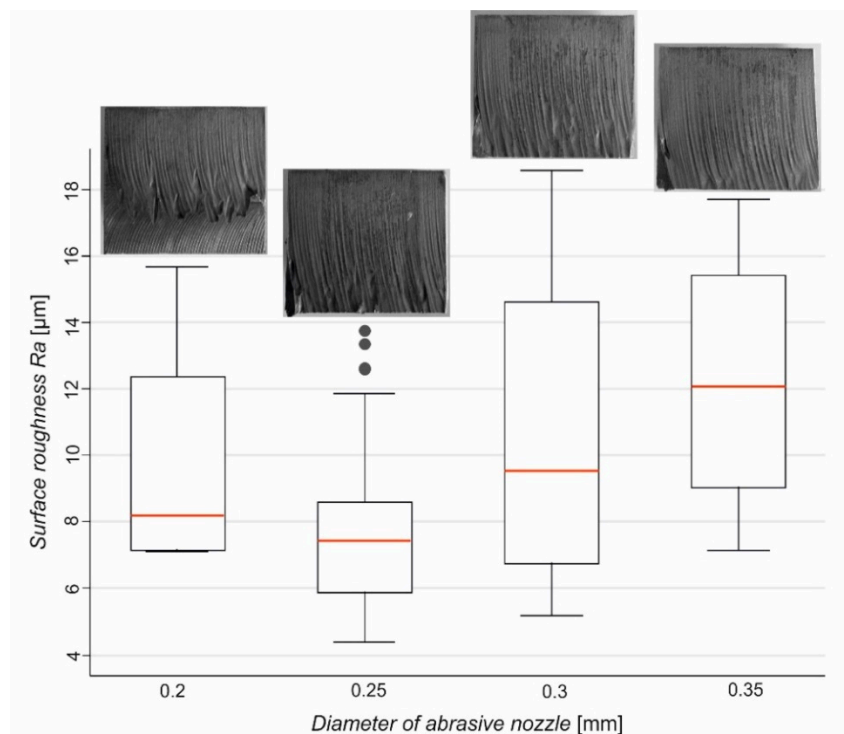


Figure 6. Effect of abrasive nozzle diameter on the surface roughness value Ra .

On the interpretation and justification of cross-correlations and the model (10): the members (products of parameters) in the concerned Equation (10) express correlations between pairs of significant parameters, namely correlations of physical significance for the used AWJ technology.

The product $x_1 \cdot x_5$ in Equation (10) represents the area velocity v_A , dimensionally corresponding to:

$$x_1 \cdot x_5 = [L] \cdot [v_p] = \text{mm} \cdot \text{mm} \cdot \text{min}^{-1} = \text{mm}^2 \cdot \text{min}^{-1}$$

The product in Equation (10) represents the volume flow rate Q_V for time t as the volume of liquid for time flowing through one place (the whole cross-section at one point (tubes, nozzles) per a time unit):

$$x_1 \cdot (x_5)^2 = [L] \cdot [(v_p)^2] = \text{mm} \cdot \text{mm}^2 \cdot \text{min}^{-2} = \text{mm}^3 \cdot \text{min}^{-2}$$

The total effect of v_A and Q_V over time presents not only the isolated effects of the distance of the nozzle outlet from the machined surface, but their combination in the sense that the resulting value should not be extreme (maximum, minimum), but optimal with respect to the desired roughness value. The product $x_3 \cdot x_4$ in Equation (11) represents the square of the mass flow rate Q_m related to the distance of the nozzle outlet from the surface to be treated, dimensionally corresponding to:

$$x_3 \cdot x_4 = [Q_V] \cdot [m_a] = \text{l} \cdot \text{min}^{-1} \cdot \text{g} \cdot \text{min}^{-1} = \text{g}^2 \cdot \text{min}^{-2}$$

The total effect of the subject product $x_3 \cdot x_4$ also presents not only the isolated effects of the volume flow rate and the amount of abrasive but their combination in the sense that the resulting value should not be extreme but again optimal in relation to the required roughness.

A graphical representation of the variation of the surface roughness value Ra from the change in the cutting head feed rate and the abrasive mass flow is shown in Figure 7. The graph shows that the minimum values of the studied variable Ra can be achieved by low cutting head speeds and high abrasive mass flow values. If the abrasive mass flow value is maintained at the upper limit of the experimentally used interval and the value of the feed rate is gradually increased, the value of the studied parameter Ra will also increase up to 6 μm . Such an adjustment of the processing system

guarantees minimum surface roughness values at a nozzle/material distance of 3 mm, abrasive nozzle diameter of 0.25 mm, and a material thickness of 15 mm. The function reaches its maximum in the area of cutting head feed rate and the lower value of abrasive mass flow within the range of experimentally used values. In this area, the value of the studied parameter Ra reaches the value of almost 16 μm , which represents an increase of more than 530% compared to the minimum values of the investigated parameter at the lower limit of the used speed range, cutting head feed, and upper abrasive mass flow interval.

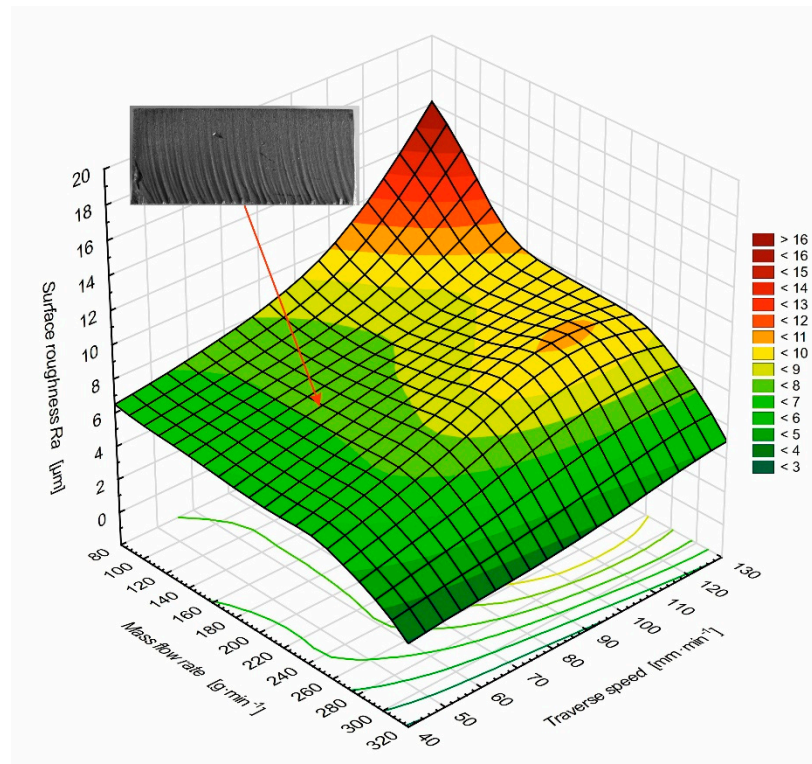


Figure 7. Dependence of surface roughness Ra on the variation of cutting head feed rate and abrasive mass flow.

The dependence of the surface roughness value Ra on the variation of the cutting head feed rate and flow of the high-pressure water is shown in Figure 8.

The minimum surface roughness achieved is in the narrow range of low cutting head feed rates and high-pressure water flow rates in the range of 1.65–3.25 $\text{l}\cdot\text{min}^{-1}$, where surface roughness values Ra are less than 5 μm . By increasing the cutting head feed rate to the maximum value of the experimental range used (Table 4) and the maximum value of the high-pressure water flow, the surface roughness value reaches its maximum at almost 24 μm .

3.3. Interpretation of Obtained Results and Design of Using them for the Application Sphere

Given the increased requirements regarding cutting and competitiveness, other ways to improve performance have begun to be searched without increasing the shifts of operation. Combinations of high-pressure water flow rates were chosen so that splitting the jet affects the cutting performance to the smallest possible extent. The maximum consumption of 3.5 l of high-pressure water according to the consumption in the usual practice was taken into account.

Based on the stated measurement data, their evaluation, analysis, interpretation, and the created prediction model, the user-desired quality of the cut surface can be achieved, with a corresponding change in the input parameters (according to the prediction model). The prediction model, which was not created analytically, but purely statistically (10), has a physically informative value mainly through

its interaction members. The respective correlation products of the parameters have the physical significance of the surface velocity, the volume flow rate relative to time, and the square of the mass flow relative to the distance of the nozzle outlet from the surface to be treated.

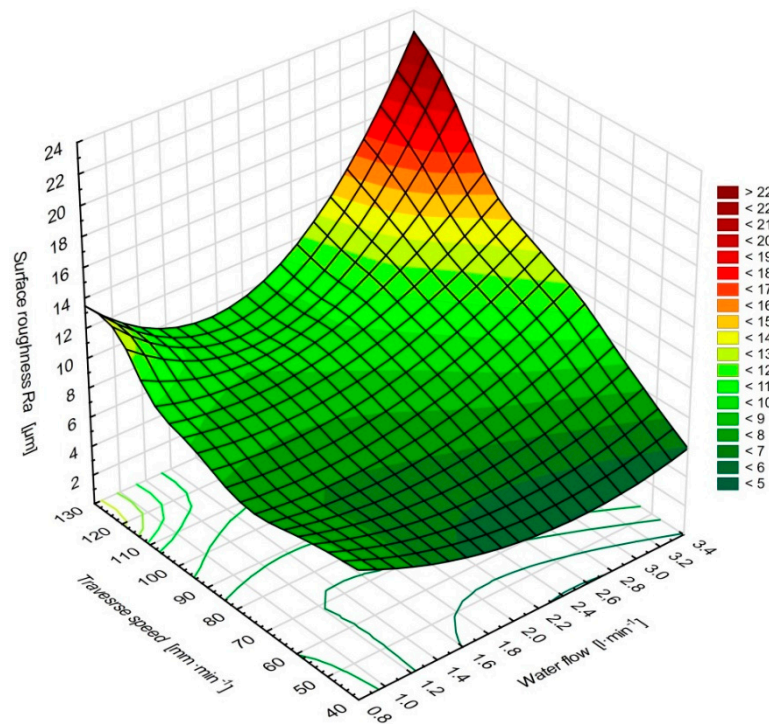


Figure 8. Dependence of surface roughness Ra on the variation of cutting head feed rate and high-pressure water flow.

3.4. Proposal for the Classification of the Predicted Cut Quality and Recommendations Based on the Prediction Model

The results obtained in the presented publication were gradually created according to the specific requirements of customers from practice. The current methods of designing the main technological parameters of the AWJ technology process are still performed only on the basis of the subjective experience of the technologist. The optimal values of the input parameters (especially pump pressure, different cutting head feed rates, abrasive mass flow, abrasive type and size) are therefore chosen empirically, most often according to the achieved depth of division and visual condition of the test sample dividing wall.

Of the theoretical solutions, the calculations according to Hashish [37], Zeng [38], and Wang [39] are closest to the practical requirements of the technologist, but these solutions are difficult to apply in practice because they require a number of theoretical assumptions and constants that cannot be measured in practice. An exact calculation method that can be easily and quickly used in practice has not yet been developed for this technology. At present, some programs serving as technological aids are already available, but they can only be used to get an approximate idea, i.e., they are not based on realistically measured technological parameters of AWJ technology of divisibility of the type of required material. They relate to a very limited number of technological parameters and address the technological properties of the divided material insufficiently. The mechanical properties of each material, which enter into technological calculations, show such considerable differences that the tabular values of these parameters should also be considered as approximate. Based on the above reasons, a uniform technological classification of technical materials is still missing, both according to deformation parameters and according to optimal technological parameters. The combination of water

and abrasive nozzle flow ratios was studied to predict the quality of the cut in relation to the weight of abrasive for hydro-erosive flow (Tables 12 and 13).

Table 12. Standard and proposed nozzle (jet) configurations.

Water Nozzles [mm]	Focusing Nozzles Recommended by the Manufacturer [mm]	Focusing Nozzles Designed and Verified in WATTING Prešov [mm]
0.20	0.76	0.76 or 1.02
0.25	0.76 or 0.90	0.76 or 1.02
0.30	0.90	0.76 or 1.02
0.35	1.10	0.76 or 1.02

Table 13. Sizing variants for splitting water jet.

Water Nozzles Number	Focusing Nozzles Recommended by the Manufacturer [mm/mm/l·min ⁻¹]	Focusing Nozzles Designed and Verified in WATTING Prešov [mm/mm/l·min ⁻¹]
1.	0.20/0.76/1.05	0.20/0.76/1.05
2.	0.20/0.76/1.05	0.25/0.76/1.65
3.	0.20/0.76/1.05	0.30/0.76/2.37
4.	0.25/0.76/1.65	0.25/0.76/1.65
	or	
5.	0.20/1.02/1.05	0.20/1.02/1.05
6.	0.20/1.02/1.05	0.25/1.02/1.65
7.	0.20/1.02/1.05	0.30/1.02/2.37
8.	0.25/1.02/1.65	0.25/1.02/1.65
	other possibilities	
9.	0.20/0.76/1.05	0.20/1.02/1.05
10.	0.20/0.76/1.05	0.25/1.02/1.65
11.	0.25/0.76/1.65	0.25/1.02/1.65

Based on the verification of the prediction model (10), for all four categories, the following can be recommended:

- For a material thickness of 0.1–5 mm, the roughness of 1–6.3 μm is guaranteed, abrasive 130 $\text{g}\cdot\text{min}^{-1}$,
- For a material thickness of 5–20 mm, the roughness of 3.2–12.5 μm is guaranteed, abrasive 180 $\text{g}\cdot\text{min}^{-1}$,
- For a material thickness of 21–50 mm, the roughness of 6.3–25 μm is guaranteed, abrasive 250 $\text{g}\cdot\text{min}^{-1}$,
- For a material thickness of 51–80 mm, the roughness of 12.5–40 μm is guaranteed, abrasive 300 $\text{g}\cdot\text{min}^{-1}$ (usually without roughness guarantee for cutting with an allowance),
- For a material thickness of over 80 mm, cutting with an allowance, abrasive 350 $\text{g}\cdot\text{min}^{-1}$.

The optimal set of factors were identified from a physical, technological, and technical point of view in relation to the quality and productivity of the hydro-abrasive erosion process. The impact of technical factors on the hydro-abrasive manufacturing process largely affects the continuity of the manufacturing process, so the whole complex of these factors can significantly affect the overall productivity of the manufacturing process. The decisive factors are water specification, hydraulic and high-pressure systems, as well as the choice of water and abrasive nozzles.

The publication also provides specific recommendations for practice based on the specific requirements of customers from practice based on the achieved results according to the prediction model (10):

1. Recommendations for a group of materials of austenitic steels 30 mm thick:

- For a thickness of 0.1–5 mm, a roughness of 1–3.2 μm , a speed of 250–800 $\text{mm}\cdot\text{min}^{-1}$ is guaranteed,
- For a thickness of 5–10 mm, a roughness of 3.2–12.5 μm , a speed of 110–250 $\text{mm}\cdot\text{min}^{-1}$ is guaranteed,
- For a thickness of 10–20 mm, a roughness of 6.3–12.5 μm , a speed of 70–110 $\text{mm}\cdot\text{min}^{-1}$ is guaranteed,
- For a thickness of 20–30 mm, a roughness of 6.3–15 μm , a speed of 25–70 $\text{mm}\cdot\text{min}^{-1}$ is guaranteed.

Recommendation of constant parameters for the following stated material thicknesses:

- Water flow 0.25 mm,
- Abrasive weight max. 200 g·min⁻¹,
- Abrasive nozzle 0.76 mm,
- Water pressure 300 MPa.

2. Recommendations for the group of materials of austenitic steels with a thickness of 30–150 mm:

- For a thickness of 30–50 mm, a roughness of up to 25 µm is guaranteed (for many cutting operations with allowance, without a guarantee of roughness),
- For a thickness of 50–80 mm, a roughness of operations 25–40 µm is guaranteed (usually without a roughness guarantee for cutting with allowance),
- For a thickness of the material over 80 mm with allowance,
- For a thickness of 80–150 mm a roughness greater than 40 µm (usually without roughness guarantee for cutting with allowance).
- Recommendation of constant parameters for the following stated material thickness:
- Water flow 1.65–2.37 l·min⁻¹,
- Abrasive weight up to 250–350 g·min⁻¹,
- Abrasive nozzle 1.02 mm,
- Water pressure 350 MPa,
- Cutting speed up to 100 mm·min⁻¹ depending on the nature of the requirement and the nature of the use of the product.

Recommendations for practice:

- Lower cutting speed, i.e., max. 2/3 of the cutting speed;
- The lowest lift of the cutting head above the material 3 mm, with the optimum lift being 2 mm above the material (in practice a range of 3 to 7 mm, usually 4 mm, is used),
- Smaller inner diameter of the abrasive nozzle 0.76 mm, for better focusing of the jet,
- Flow rates of 1.05 and 1.65 l·min⁻¹ are suitable for thicknesses up to 20 mm,
- Weight of abrasive 150–200 g·min⁻¹ is suitable for material thickness up to 20 mm,
- For larger material thicknesses up to 80 mm, larger flow rates of 2.37 to 3.25 l·min⁻¹ are suitable, and the abrasive weight per head is 200, 250, 300 g·min⁻¹,
- Larger inner diameter of the abrasive nozzle 1.02–1.1 mm, suitable for materials up to a thickness of 80 mm,
- The total assumptions of the roughness of the cut surface according to the groups of material thickness are for the thickness:

0.1–5 mm, assumption of roughness 1–6.3 µm;

5–20 mm, assumption of roughness 3.2–12.5 µm;

21–50 mm, assumption of roughness 6.3–25 µm (usually without roughness guarantee for cutting with allowance);

51–80 mm assumption of roughness 12.5–40 µm (usually without guarantee of roughness for cutting with allowance);

for material thicknesses over 80 mm, cutting with an allowance.

4. Conclusions

The expected result of the presented publication is the confirmation of the theoretical-qualitative assumption that the basic operating parameters of AWJ have a direct and measurably significant effect

on the roughness of the generated surface. The investigated material was austenitic steel AISI 304, which is currently the most widespread type of anti-corrosion material in technical practice.

The prediction model (10) of the surface structure generated by the abrasive water jet was created and verified based on the determined dependence of the roughness parameter Ra on the input technological parameters: high-pressure water volume flow, abrasive nozzle diameter, nozzle distance from the material surface, cutting head feed rate, abrasive mass flow, and material thickness. The effects of these six parameters on surface roughness were investigated based on the targeted experimental procedures. The results of the presented measurements were processed by statistical methods, while the predictive statistical model was created with a sensitivity of 5%.

In recent years, the demands on industrial cutting processes have increased significantly. Not only is it necessary to improve the quality of the created cut surface, but also to increase the production and significantly reduce the cost of the production process. The presented application was solved in Slovak companies WATTING Ltd. (Budovateľská 3598/38, 080 01 Prešov, Slovakia) and FEDSTROJ Ltd. (Urbárska 16 040 18 Košice-Krásna, Slovakia), which manufacture components for the assembly of various types of double-walled containers for liquid gases.

The publication also makes specific recommendations for practice based on the specific requirements of customers from practice, based on the results achieved according to the prediction model (10). Since a uniform technological classification of technical materials is still missing, both according to the deformation parameters and according to the optimal technological parameters, a proposal for the classification of the predicted cut quality is also presented. Further scientific-research continuity can be expected in the future, especially in connection with the verification of the dependence of the roughness of machined surfaces on the input technological parameters of other frequented materials in engineering practice and also in connection with increasing AWJ efficiency as a promising and flexible technology.

Author Contributions: Conceptualization, J.K. (Jan Kmec) and M.G.; methodology, M.H. and J.V.; validation, M.K. (Milena Kušnerová), M.K. (Monika Karková) and M.K. (Milan Kadnár); formal analysis, A.V.; investigation, J.K. (Jan Kmec), M.H., J.V. and M.G.; data curation, J.K. (Jiří Kříž) and M.K. (Milan Kadnár); writing—original draft preparation, J.K. (Jan Kmec); writing—review and editing, M.H., M.K. (Milena Kušnerová), M.G., J.V.; funding acquisition, M.H. All authors have read and agreed to the published version of the manuscript.

Funding: This publication was created within the project SVV201905 granted by Ministry of Education, Youth and Sports of the Czech Republic and grant agency of the Slovak University of Agriculture in Nitra GA 7/19.

Conflicts of Interest: The authors declare no conflict of interest.

Nomenclature

A_5	ductility	[%]
d_a	diameter of abrasive nozzle	[mm]
d_o	diameter of the water jet	[mm]
h	thickness of cut material	[mm]
HB	hardness	[-]
KCU	notch strength	[J·cm ⁻²]
L	distance of the nozzle from the material surface	[mm]
m_a	mass flow of abrasive	[g·min ⁻¹]
p	high-pressure water pressure	[MPa]
ρ	density of liquid medium	[kg·m ⁻³]
Ra	mean arithmetic deviation of the profile	[μm]
$Rp_{0.2}$	yield strength	[MPa]
Rm	breaking strain	[MPa]
v	flow rate	[m·s ⁻¹]
v_p	cutting head feed rate	[mm·min ⁻¹]
v_A	areal velocity	[mm ² ·min ⁻¹]
Q_V	volume flow rate	[l·min ⁻¹]
Q_m	mass flow	[g·min ⁻¹]

References

- Henning, A.; Liu, H.T.; Olsen, C. Economic and technical efficiency of high-performance abrasive waterjet cutting. *J. Press Vessel Technol.* **2012**, *134*, 021405. [\[CrossRef\]](#)
- Folkes, J. Waterjet-an innovative tool for manufacturing. *J. Mater. Process. Technol.* **2009**, *209*, 6181–6189. [\[CrossRef\]](#)
- Kovacevic, R.; Hashish, M.; Mohan, R.; Ramulu, M.; Kim, T.J.; Geskin, E.S. State of the art of research and development in abrasive waterjet machining. *J. Manuf. Sci. Eng.* **1997**, *119*, 776–785. [\[CrossRef\]](#)
- Liu, H.T. Waterjet technology for machining fine features pertaining to micromachining. *J. Manuf. Process.* **2010**, *12*, 8–18. [\[CrossRef\]](#)
- Miller, D.S. Micromachining with abrasive waterjets. *J. Mater. Process. Technol.* **2004**, *149*, 37–42. [\[CrossRef\]](#)
- Junkar, M.; Jurisevic, B.; Fajdiga, M.; Grah, M. Finite element analysis of single particle impact in abrasive water jet machining. *Int. J. Impact Eng.* **2006**, *32*, 1095–1112. [\[CrossRef\]](#)
- El-hofy, H. *Advanced Machining Processes: Nontraditional and Hybrid Machining Processes*, 1st ed.; McGraw Hill Professional: New York, NY, USA, 2005; p. 253.
- Vikram, G.; Ramesh, B.N. Modelling and analysis of abrasive water jet cut surface topography. *Int. J. Mach. Tools Manuf.* **2002**, *42*, 1345–1354. [\[CrossRef\]](#)
- Wang, J. Predictive depth of jet penetration models for abrasive water jet cutting of alumina ceramics. *Int. J. Mech. Sci.* **2007**, *49*, 306–316. [\[CrossRef\]](#)
- Dumbhare, P.A.; Dubey, S.; Deshpande, Y.V.; Andhare, A.B.; Barve, P.S. Modelling and Multi-Objective Optimization of Surface Roughness and Kerf Taper Angle in Abrasive Water Jet Machining of Steel. *J. Braz. Soc. Mech. Sci. Eng.* **2018**, *40*, 259. [\[CrossRef\]](#)
- Kök, M.; Kanca, E.; Eyercioğlu, Ö. Prediction of surface roughness in abrasive waterjet machining of particle reinforced MMCs using genetic expression programming. *Int. J. Adv. Manuf. Technol.* **2011**, *55*, 955–968. [\[CrossRef\]](#)
- Yu, Y.; Sun, T.; Yuan, Y.; Gao, H.; Wang, X. Experimental investigation into the effect of abrasive process parameters on the cutting performance for abrasive waterjet technology: A case study. *Int. J. Adv. Manuf. Tech.* **2020**, *107*, 2757–2765. [\[CrossRef\]](#)
- Kovacevic, R. Monitoring the depth of abrasive waterjet penetration. *Int. J. Mach. Tool Manu.* **1992**, *32*, 725–736. [\[CrossRef\]](#)
- Hashish, M. Optimization factors in abrasive waterjet machining. *Trans. ASME J. Eng. Ind.* **1991**, *113*, 29–37. [\[CrossRef\]](#)
- Jegaraj, J.J.R.; Babu, N.R. A soft computing approach for controlling the quality of cut with abrasive waterjet cutting system experiencing orifice and focusing tube wear. *J. Mater. Process. Technol.* **2007**, *185*, 217–227. [\[CrossRef\]](#)
- Shanmugam, D.K.; Wang, J.; Liu, H. Minimization of kerf tapers in abrasive waterjet machining of alumina ceramics using a compensation technique. *Int. J. Mach. Tool Manu.* **2008**, *48*, 1527–1534. [\[CrossRef\]](#)
- Valíček, J.; Czán, A.; Harničárová, M.; Šajgalík, M.; Kušnerová, M.; Czánová, T.; Kopál, I.; Gombár, M.; Kmec, J.; Šafář, M. A new way of identifying, predicting and regulating residual stress after chip-forming machining. *Int. J. Mech. Sci.* **2019**, *155*, 343–359. [\[CrossRef\]](#)
- Valíček, J.; Harničárová, M.; Öchsner, A.; Hutyrová, Z.; Kušnerová, M.; Tozan, H.; Michenka, V.; Šepelák, V.; Mital, D.; Zajac, J. Quantifying the Mechanical Properties of Materials and the Process of Elastic-Plastic Deformation under External Stress on Material. *Materials* **2015**, *8*, 7401–7422. [\[CrossRef\]](#)
- Valíček, J.; Borovička, A.; Hloch, S.; Hlaváček, P. Method for the Design of a Technology for the Abrasive Waterjet Cutting of Materials. U.S. Patent 9,073,175, 7 July 2015.
- Hloch, S.; Valíček, J. Prediction of distribution relationship of titanium surface topography created by abrasive waterjet. *Int. J. Surf. Sci. Eng.* **2001**, *5*, 152–168. [\[CrossRef\]](#)
- Valíček, J.; Borovička, A.; Hloch, S.; Hlaváček, P. Method for the Design of a Technology for the Abrasive Waterjet Cutting of Materials Kawj. Czech Republic Patent CZ 305514 B6, 23 July 2010.
- Hloch, S.; Valíček, J. Topographical anomaly on surfaces created by abrasive waterjet. *Int. J. Adv. Manuf. Tech.* **2012**, *59*, 593–604. [\[CrossRef\]](#)
- Valíček, J.; Hloch, S.; Držík, M.; Ohlídal, M.; Mádr, V.; Lupták, M.; Fabian, S.; Radvanská, A.; Páleníková, K. Study of Surfaces Generated by Abrasive Waterjet Technology. In *Innovative Algorithms and Techniques in*

- Automation, Industrial Electronics and Telecommunications*; Sobh, T., Elleithy, K., Mahmood, A., Karim, M., Eds.; Springer: Dordrecht, The Netherlands, 2007; pp. 181–185.
24. Momber, A.W.; Kovacevic, R. *Principles of Abrasive Water Jet Machining*; Springer: New York, NY, USA, 1998.
 25. Hashish, M. Visualization of the abrasive-waterjet cutting process. *Exp. Mech.* **1998**, *28*, 159–169. [[CrossRef](#)]
 26. Hashish, M. A model study of metal cutting with abrasive water jet. *ASME J. Eng. Mater. Technol.* **1984**, *106*, 88–100, ISSN 0094-4289. [[CrossRef](#)]
 27. Orbanic, H.; Junkar, M. Analysis of striation formation mechanism in abrasive water jet cutting. *Wear* **2008**, *265*, 821–830. [[CrossRef](#)]
 28. Uthayakumar, M.; Khan, M.A.; Kumaran, S.T.; Slota, A.; Zajac, J. Machinability of nickel-based superalloy by abrasive water jet machining. *Mater. Manuf. Process.* **2016**, *31*, 1733–1739. [[CrossRef](#)]
 29. Vasanth, S.; Muthuramalingam, T.; Vinothkumar, P.; Geethapriyan, T.; Murali, G. Performance analysis of process parameters on machining titanium (Ti-6Al-4V) alloy using abrasive water jet machining process. *Procedia CIRP* **2016**, *46*, 139–142. [[CrossRef](#)]
 30. Kovacevic, R.; Mohan, R.; Beardsley, H.E. Monitoring of thermal energy distribution in abrasive waterjet cutting using infrared thermography. *J. Manuf. Sci. Eng.* **1996**, *118*, 555–563. [[CrossRef](#)]
 31. Belhocine, A.; Wan Omar, W.Z. An analytical method for solving exact solutions of the convective heat transfer in fully developed laminar flow through a circular tube. *Heat Transf. Asian Res.* **2017**, *46*, 1342–1353. [[CrossRef](#)]
 32. Belhocine, A.; Abdullah, O.I. Numerical simulation of thermally developing turbulent flow through a cylindrical tube. *Int. J. Adv. Manuf. Technol.* **2019**, *102*, 2001–2012. [[CrossRef](#)]
 33. Natarajan, Y.; Murugesan, P.K.; Mohan, M.; Khan, S.A.L.A. Abrasive Water Jet Machining process: A state of art of review. *J. Manuf. Process.* **2020**, *49*, 271–322. [[CrossRef](#)]
 34. Marshall, P. *Austenitic Stainless Steels: Microstructure and Mechanical Properties*; Elsevier Applied Science Publishers: London, UK, 1984; p. 432.
 35. Mahoney, M.; Magel, R. Estimation of the power of the Kruskal-Wallis test. *Biometrical J.* **1996**, *38*, 613–630. [[CrossRef](#)]
 36. Hecke, T.V. Power study of ANOVA versus Kruskal-Wallis test. *J. Stat. Manag. Syst.* **2012**, *15*, 241–247. [[CrossRef](#)]
 37. Hashish, M. Prediction models for AWJ machining operations. In Proceedings of the 7th American Water Jet Conference, Seattle, WA, USA, 28–31 August 1993; Hashish, M., Ed.; Water Jet Technology Association: St. Louis, MO, USA, 1993; pp. 205–216.
 38. Zeng, J.; Kim, T. Parameter prediction and cost analysis in abrasive waterjet cutting operations. In Proceedings of the 7th American Water Jet Conference, Seattle, WA, USA, 28–31 August 1993; Hashish, M., Ed.; Water Jet Technology Association: St. Louis, MO, USA, 1993; pp. 28–31.
 39. Wang, J. A new model for predicting the depth of cut in abrasive waterjet contouring of alumina ceramics. *J. Mater. Process. Technol.* **2009**, *209*, 2314–2320. [[CrossRef](#)]

